Glass homogeneity effect on wavefront aberration in lithography projection lens

Hongbo Shang (尚红波)*, Wei Huang (黄 玮), Chunlai Liu (刘春来), Weicai Xu (许伟才), and Wang Yang (杨 旺)

State Key Laboratory of Applied Optics, Changchun Institute of Optics, Fine Mechanics and Physics, Chinese Academy of Sciences, Changchun 130033, China

**Corresponding author: silverbirchs@gmail.com*

Received April 29, 2013; accepted August 2, 2013; posted online September 3, 2013

Analysis of glass homogeneity using the attaching interferometric data model neglects body distribution. To improve analysis accuracy, we establish the three-dimensional gradient index (GRIN) model of glass index by analyzing fused silica homogeneity distribution in two perpendicular measurement directions. Using the GRIN model, a lithography projection lens with a numerical aperture of 0.75 is analyzed. Root mean square wavefront aberration deteriorates from 0.9 to 9.65 nm and then improves to 5.9 nm after clocking.

OCIS codes: 080.3095, 220.3740, 220.1000.
doi: 10.3788/COL201311.090802.

A lithography projection lens can simultaneously achieve a large field and numerical aperture (NA) and has an extremely high image resolution. To meet rigorous imaging demands, strict tolerances and various compensation methods are required. Among all such tolerances, glass homogeneity error may seriously degrade image quality. Thus, the effects of this error should be accurately analyzed and compensated. Liao et al.[1] proposed an approach of simplifying glass homogeneity distribution that considers the fourth and ninth fringe Zernike polynomials. However, other components of fringe Zernike polynomials such as coma, astigmatism, and trefoil can also deteriorate the image quality and are usually more difficult to be compensated. In this letter, we discuss an accurate method of analyzing glass homogeneity effects on optical systems. Glass homogeneity distribution is simulated as gradient index distribution (the gradient index (GRIN) model), and its three-dimensional (3D) model is established by analyzing homogeneity measurement data of fused silica. We then take an NA0.75 projection lens as an example to analyze wavefront degradation caused by glass homogeneity. We likewise present compensation results by clocking lens elements.

Glass blank index homogeneity can be measured with an interferometer[2,3]. The wavefront map of measurement is the optical path (OP) difference caused by index homogeneity[4,5]. We can use fringe Zernike polynomials to express the wavefront error as

$$\Delta w(x,y) = \Delta w(\rho,\theta) = \sum_{i=1}^{36} c_i\, z_i(\rho,\theta), \tag{1}$$

where $z_i(\rho,\theta)$ is the base function of fringe Zernike polynomials.

For simplicity, we generally conduct analysis by attaching interferometric data of glass homogeneity to lens surface (the attaching interferometric data (AID) model) when examining the effect of index homogeneity on the optical system. This technique provides only an approximate result because it does not consider real ray paths when rays trace through the lens, as the red light shows in Fig. 1. An accurate OP needs to be calculated by[6]

$$OP = \int n \mathrm{d}s, \tag{2}$$

where $n(x,y,z)$ is the glass index associated with position (x,y,z), and $\mathrm{d}s = \sqrt{x^2+y^2+z^2}$ is the arc length along the ray path. As a result of inhomogeneous distribution, fused silica can be considered as the gradient index material (the GRIN model), and light path through the lens is determined by[7]

$$\frac{\mathrm{d}}{\mathrm{d}s}\left[n(\mathbf{r})\frac{\mathrm{d}\mathbf{r}}{\mathrm{d}s}\right] = \nabla n(\mathbf{r}), \tag{3}$$

where $\mathbf{r} = x\cdot\vec{i} + y\cdot\vec{j} + z\cdot\vec{k}$ is the light transmission position vector.

To use an actual ray trace to accurately analyze wavefront error contribution caused by index homogeneity in projection lens, we need to create a volume index distribution. Assuming that the thickness of the glass blank

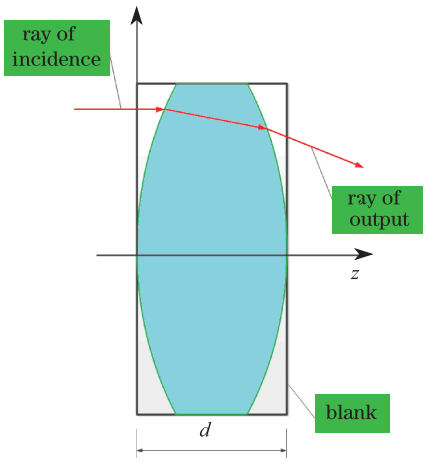

Fig. 1. Real ray path through lens.

is d, the index volume distribution is $n(x, y, z)$, and the nominal glass index is n_0, then the wavefront error measured with the interferometer is

$$\Delta w(x, y) = \int_0^d n(x, y, z)\mathrm{d}z - n_0 d, \tag{4}$$

where $\Delta w(x,y)$ is represented by Eq. (1).

Glass index homogeneity data are obtained from normal and edge side directions of the glass blank to determine $n(x,y,z)$, as illustrated in Fig. 2. A measurement result of fused silica blank is shown in Fig. 3. Power is not removed because it is produced by the material.

Based on the measurement results of Figs. 3(a) and (b), we determine that compared with the index homogeneity distribution along the radial direction, the index homogeneity distribution along the axial direction is approximately uniform and can be considered as a linear distribution:

$$\Delta n\,(z) = a + k \cdot z, \tag{5}$$

where Δn(z) is the index variety along the axial direction, k is the slope, a is the constant, and z is the coordinate along the axial direction.

Thus, the body index distribution $n(x,y,z)$ can be simplified as

$$n(x, y, z) = n(x, y) + k \cdot z, \tag{6}$$

a in Eq. (5) is included in $n(x,y)$.

We select three groups of index homogeneity data along the axial direction in Fig. 3(b) and fit them using Eq. (5) respectively. The fitting results of a and k are listed in Table 1. Based on these results, we can approximate that $k = 0$ in subsequent analyses.

After integrating Eq. (6) with Eq. (4), we obtain

$$n\,(x, y, z) = \frac{\Delta w(x, y)}{d} + n_0. \tag{7}$$

Now, the actual ray can be traced using Eq. (3).

Based on the results of the aforementioned analysis, we adopt the user-defined material interface of the commercial software CODE V[8] and write codes to establish an accurate index distribution model. Notably, the GRIN model directly uses the homogeneity measurement map because it can locate the lens in the blank according to the ray's coordinate, as shown in Fig. 1.

A lithography projection lens with NA = 0.75 working at 193 nm is used for our analysis, as shown in Fig. 4[9].

The entire system is composed of 20 lenses and made of fused silica. The design exit pupil wavefront error distribution after the subtraction of best-fit power is shown in Fig. 5. System aberration is well corrected, and the root mean square (RMS) wavefront error values of all fields are <0.9 nm.

Degradation of wavefront error caused by index homogeneity and its compensation calculated by the GRIN model are shown in the following section.

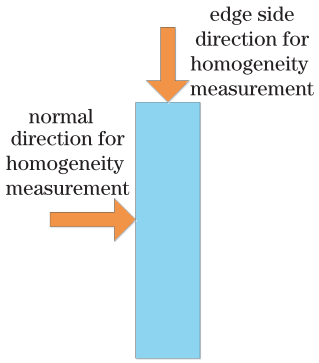

Fig. 2. Measurement direction of a glass blank.

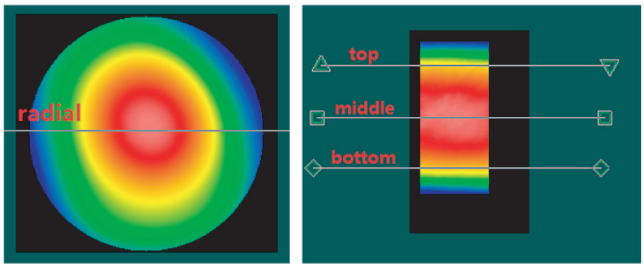

(a) (b)

Fig. 3. (a) Normal direction measurement result (radial distribution) and (b) edge side measurement result (axial distribution).

Table 1. Fitting Results

	Data	a (ppm)	k
Axial Data	Top	0.2984	7.31×10^{-5}
	Middle	0.4360	-3.20×10^{-6}
	Bottom	0.2915	-2.02×10^{-5}

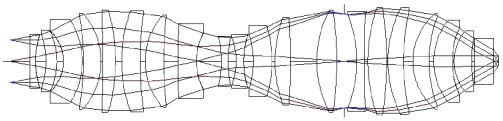

Fig. 4. A NA0.75 projection lens.

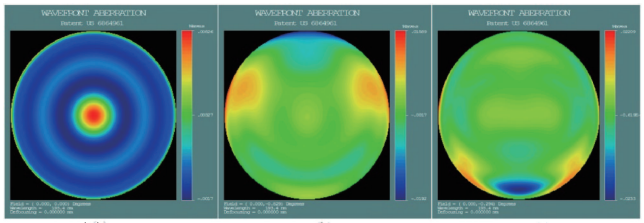

(a) (b) (c)

Fig. 5. Design exit pupil wavefront error distribution: (a) field 0, RMS = 0.67 nm; (b) field 0.5, RMS = 0.82 nm; (c) field 1, RMS = 0.89 nm.

We choose 20 homogeneity measurement data of glass blanks for analysis. Wavefront error distribution is shown in Fig. 6. Compared with Fig. 5, we can determine that index homogeneity induces the system wavefront to significantly deteriorate, with a maximum RMS value reaching up to 9.65 nm.

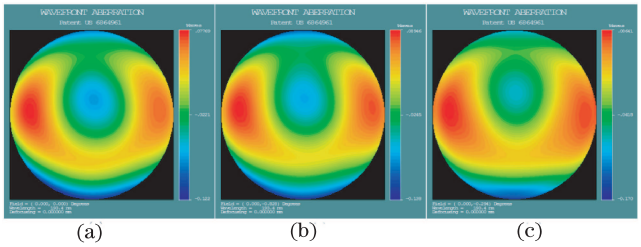

(a) (b) (c)

Fig. 6. Exit pupil wavefront error distribution caused by glass homogeneity: (a) field 0, RMS = 7.97 nm; (b) field 0.5, RMS = 9.26 nm; (c) field 1, RMS = 9.65 nm.

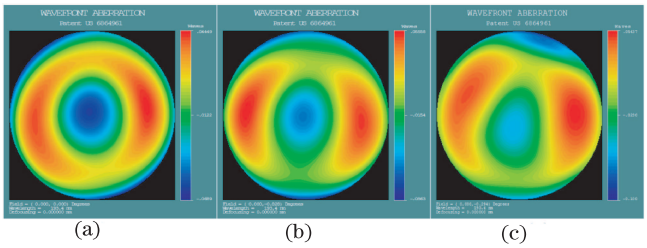

(a) (b) (c)

Fig. 7. Exit pupil wavefront error distribution after clocking: (a) field 0, RMS = 5.16 nm; (b) field 0.5, RMS = 5.78 nm; (c) field 1, RMS = 5.90 nm.

Table 2. Zernike Terms of Wavefront Aberration Before and After Clocking

	Before Clocking			After Clocking		
Zernike	Field	Field	Field	Field	Field	Field
Term	0	0.5	1	0	0.5	1
5	5.53	7.15	7.72	1.20	3.23	3.52
6	0.12	0.02	0.39	1.01	0.41	1.12
7	1.02	0.91	0.87	0.35	0.35	0.77
8	2.61	2.82	3.64	0.15	0.44	1.55
9	4.78	4.72	4.06	4.78	4.54	3.85
z5 to z36	7.97	9.26	9.65	5.16	5.78	5.90

To meet the requirements on wavefront error of a projection lens, deterioration of the wavefront error caused by index homogeneity can be compensated through clocking elements[10]. By optimizing the clocking angle of each element, the wavefront error distribution is obtained, as shown in Fig. 7. The RMS value decreases to 5.9 nm, and the wavefront error after clocking is effectively reduced.

Details of wavefront aberration before and after clocking are shown in Table 2. This table lists only the values of main coefficients z5 to z9 and the RMS wavefront aberrations. They are all RMS values in the unit of nanometers. After analyzing data in Table 2, we find that nonsymmetrical coefficients except z6, which is relatively small, dramatically decrease. The main component of wavefront aberration after clocking is spherical aberration, which can be compensated by adjusting spaces between elements in lens during the assembly process.

In conclusion, we analyze the defects of the AID model, propose the GRIN model to simulate index homogeneity, and establish a 3D index distribution after analyzing the radial and axial index distributions of fused silica. We analyze index homogeneity effects on an NA0.75 projection lithography lens. We find that the system RMS wavefront deteriorates from 0.9 to 9.65 nm and then improves to 5.9 nm after clocking compensation. The methods proposed in this letter can be used to deal with more complex index distribution problems.

This work was supported by the Major National Science and Technology Project of China (No. 2009ZX02205).

References

1. Z. Liao, T. Xing, and H. Zhu, Proc. SPIE **7656,** 866846 (2010).
2. L. Deck, Appl. Opt. **42,** 2354 (2003).
3. Zygo, MST PSurf and MST PHom MetroPro Applications (2003).
4. H. Liu, Chin. Opt. Lett. **10,** 071201 (2012).
5. H. Shen, R. Zhu, Z. Gao, E. Pun, W. Wong , and X. Zhu, Chin. Opt. Lett. **11,** 032201 (2013).
6. A. Sharma, Appl. Opt. **24,** 4367 (1985).
7. M. Born and E. Wolf, *Principle of Optics,* 7th ed. (Cambridge University Press, 1999).
8. Synopsys, Inc. CODE V Electronic Document Library, version 10.5 (2012).
9. Y. Omura, "Projection exposure methods and apparatus, and projection optical systems", U.S. patent 6,864,961B2 (2005).
10. T. Matsuyama, I. Tanaka, T. Ozawa, K. Nomura, and T. Koyama, Proc. SPIE **5040,** 801 (2003).